Available online at www.sciencedirect.com
ScienceDirect
International Journal of Heat and Fluid Flow 27 (2006) 748–755
International Journal of HEAT AND FLUID FLOW
www.elsevier.com/locate/ijhff

Active control of turbulent separated flows over slanted surfaces

A. Brunn *, W. Nitsche

Department of Aerodynamics, Institute of Aeronautics and Astronautics, Technical University, Berlin 10587, Germany

Received 3 October 2005; received in revised form 23 January 2006; accepted 4 March 2006
Available online 15 June 2006

Abstract

The experimental investigations in the present paper deal with the excitation of fundamental instability mechanisms in separated free shear layers on a bluff body and downstream of a diffuser by means of periodic forcing in order to reduce the expansion of flow separation. The experiments focus on a unique approach to separation control using fundamental frequencies for local forcing in two different shear layer configurations (inner and outer diffusers). Each separation process is characterized by the periodic occurrence of large spanwise vortex structures. These vortices scale with the difference in height between the ramp ends. The excitation of these large scale vortex structures by periodic forcing intensifies the momentum transfer between the separation region and the outer flow, resulting in a substantial reduction of the reattachment length. For the inner and outer diffuser configurations, a universal value for the optimum forcing frequency was established.

Keywords: Active separation control; Bluff bodies; Channel flows; Vortex-shedding; Particle image velocimetry

1. Introduction

Flow separation from solid surfaces occurs in a variety of technical applications, such as expanding flow channels (diffusers) or car and train tails, in turbomachinery, on airfoils at high angles of attack etc. This inevitably leads to a significant decrease in efficiency (e.g., Hucho, 2002; Leder, 1992). Both active and passive methods of flow control can be applied to avoid or reduce this type of separation-induced performance loss (Lin et al., 1990; Yoshioka et al., 1999; Brunn and Nitsche, 2002 etc.) Nevertheless, practical applications are almost too complicated for an accurate analysis of these typical phenomena. Hence, generic models with the most important boundary conditions are frequently used.

An overcritical diffuser is the simplest geometry for studying flow separation phenomena. The separation process is characterized by the periodic occurrence of vortex structures. Fig. 1 shows the development of these structures in principle (Brunn, 2003): The initial Kelvin–Helmholtz-Instability (KHI) leads to a roll-up of small spanwise vortices caused by low pressure and vorticity fluctuations. These structures grow rapidly and are finally shedded from the separation region (vortex-shedding). The pressure fluctuations resulting from the shedding process propagate upstream and are reabsorbed close to the separation point, generating vorticity fluctuations, which enhance the shear layer roll-up (Kiya et al., 1997).

Investigations on active separation control in plane and axisymmetric diffusers (e.g., Brunn and Nitsche, 2002) or on simple bluff body geometries (Sigurdson, 1995; Kiya et al., 1997 etc.) were conducted successfully using forcing frequencies in the range of the observed shear layer instabilities. In these experiments wall embedded actuators were used to generate periodical perturbations, which significantly reduce the separation length.

Nevertheless, the more complicated the configuration is, the more complicated the flow structures become. This is

* Corresponding author. Tel.: +49 3031421559; fax: +49 3031422955.
E-mail address: Andre.Brunn@TU-Berlin.DE (A. Brunn).

0142-727X/$ - see front matter © 2006 Elsevier Inc. All rights reserved.
doi:10.1016/j.ijheatfluidflow.2006.03.006

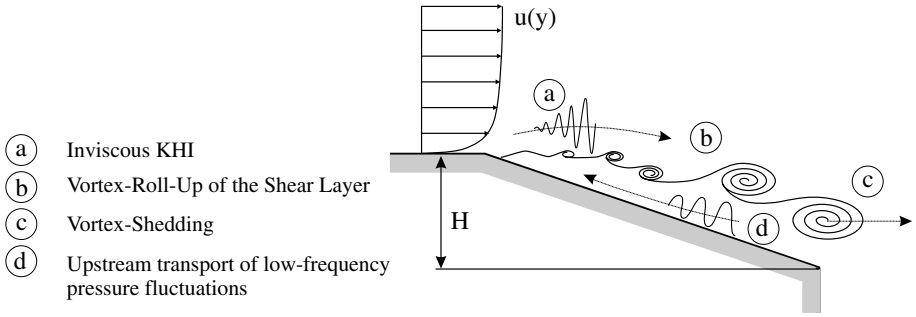

Fig. 1. Feedback-mechanism of instabilities in a separated shear layer (Brunn, 2003).

demonstrated, for instance, by Brunn (2003) in the transition from plane diffusors to axisymmetric configurations. Here the spanwise vortex structures, which have been shed from the separation region, lose their initial two-dimensional character in their early stages of development. It follows that the practicability of the proven control methods in complex geometries and real-flow applications has to be investigated.

The present experimental study focusses on the comparison of active separation control methods at a plane half diffuser and the flow behind a generic car model – the Ahmed Car Model (ACM, Ahmed et al., 1984). The flow control on this car model is an interesting application with respect to an increased efficiency of vehicles. The pressure drag is the major component of the total drag of a vehicle due to the flow separation at the rear end (Morel, 1978; Hucho, 2002). Consequently, a reduction of separation will result in a strongly decreased total drag. The ACM combines the essential geometrical parameters determining shape, length and position of the separation and is used as a reference for numerical and experimental investigations (e.g., Krajnovic and Davidson, 2002).

The study in hand uses the simple half diffuser configuration to demonstrate the receptivity of actuator perturbations in a quasi-two-dimensional separated shear layer in terms of frequency spectra of velocity fluctuations measured with a hot wire probe. In the second part of the study, the results of the first attempts of plane diffuser control are applied to a second, more complicated configuration to reduce the separation length behind a two-dimensional ACM and the connected total drag.

2. Experimental

The experimental investigations were conducted in two different flow channels: an open wind tunnel with a plane half diffuser as a test section for hot wire measurements in the separated shear layer to obtain fluctuation data in the time and frequency domain and a closed water channel in order to detect flow structures behind the generic car model (Ahmed-Body, Ahmed et al., 1984).

The half diffuser has an aspect ratio $AR = 10$ and a slant height of $H = 40$ mm, with the slant angle set at $\alpha = 25°$. The measurements were carried out at a Reynolds number

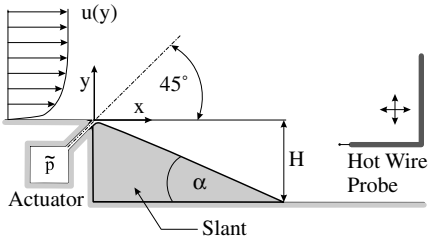

Fig. 2. Cross-section of the plane half diffuser with actuator and the hot wire probe.

based on the inflow velocity of $Re_H = 4 \times 10^4$. To reach a fully developed turbulent inlet flow, a tripping wire was placed at $100 \cdot H$ upstream the slant edge, fixing the laminar-turbulent transition far upstream. A loudspeaker-slit-actuator, situated directly at the slant edge of the diffuser, was used to generate sinusoidal pressure perturbations, and it was inclined at 45° to the mean flow direction based on the investigations of Lin et al. (1990); Yoshioka et al. (1999); Brunn (2003). A single hot wire probe was traversed in the symmetrical plane of the flow field to measure the velocity fluctuations (Fig. 2). The complete set-up is documented in the study by Brunn (2003).

The measurements at the ACM were conducted in an optically fully accessible water test section using particle image velocimetry (PIV) and digital flow visualization methods. The PIV-system consists of a frequency-doubled Nd:YAG laser, two CCD-cross-correlation-cameras to observe the near and the far wake region simultaneously and a synchronization unit (Fig. 3).

The ACM, which stretched across the whole width of the test section ($AR = B/H \approx 8$), was mounted on the channel wall with a ground clearance of $0.39 \cdot H$. The slant angle was set at $\alpha = 35°$, because observations on the fully three-dimensional model by e.g. Ahmed et al. (1984); Lienhart et al. (2002) show that the flow field of the slant region is dominated by two-dimensional spanwise vortex structures under these conditions. The initial three-dimensional flow structures at the rear side edges of the ACM should be largely suppressed through the two-dimensional stretching. All other geometrical parameters of the model are based on the original data given by Ahmed et al. (1984). The Reynolds number based on the inflow velocity and the slant

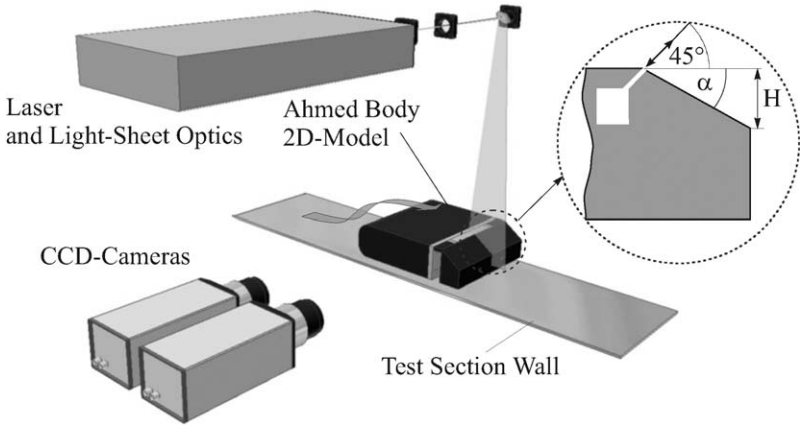

Fig. 3. Experimental Set-Up of the ACM Investigations.

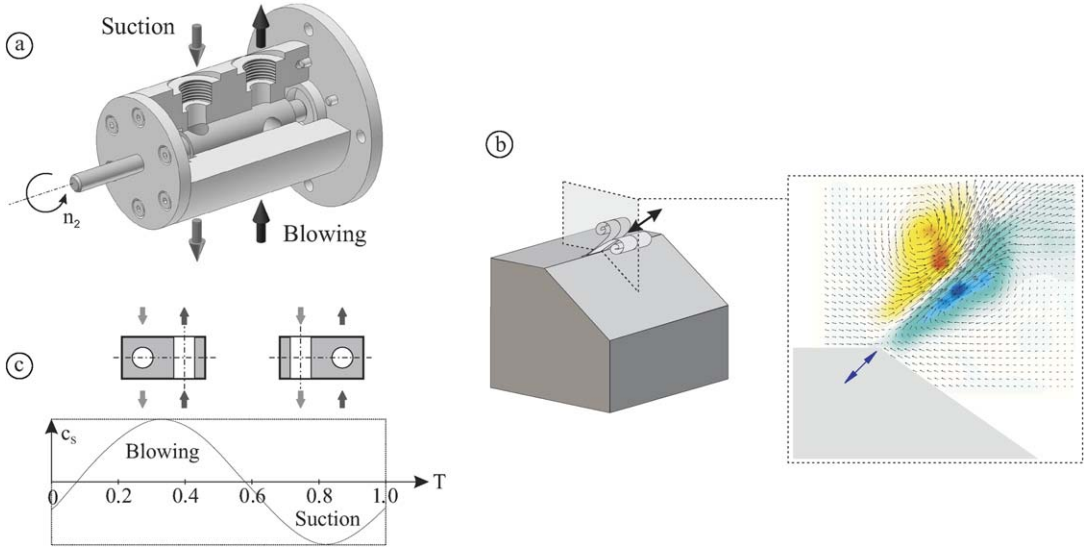

Fig. 4. Rotating valve to provide periodic perturbations ⓐ in terms of spanwise vorticity ⓑ and the perturbation amplitude c'_S for one forcing cycle T ⓒ.

height was set at 49,000. The boundary layer upstream of the car model was fully turbulent.

The periodic pressure perturbations were generated by a water pump connected to a rotating valve (Fig. 4(a)) and injected into a cavity-slit-system, resulting in an oscillating wall jet without net mass flux. The actuator is comparable to the loudspeaker slit system used at the half diffuser. Over a frequency range of $0 < St_H \leqslant 0.4$ a maximum forcing intensity of $c_\mu = 0.3 \times 10^{-3}$ could be achieved, where

$$c_\mu = \frac{A_S}{A_0} \cdot \frac{c'^2_S}{\bar{u}^2_0} \tag{1}$$

with $\bar{u}_0$ as the average velocity at the inflow, c'_S as the perturbation velocity at the slit exhaust, the cross section at the inflow A_0 and the active actuator area A_S. The perturbations during the forcing should preferably amplify the vortex structures in the separated shear layer to increase the growth of the vortices and intensify the entrainment process.

3. Results

The hot wire measurements in the plane half diffuser were carried out to obtain data of velocity fluctuations from the separated shear layer in the time and frequency domains. The RMS-distribution as well as the frequency spectra were used to describe the receptivity of the flow to periodic perturbations. Fig. 5 shows the measured spectra in the upper shear layer at different streamwise positions. Two forcing cases are compared with the unforced base flow (thick line).

These two fundamental frequencies for the vortex-shedding ($f_{S,1}$, Fig. 5(a)) and for the initial shear layer instability ($f_{S,2}$, Fig. 5(b)) were observed in earlier investigations described by Brunn (2003), where these frequencies turned out to be the most amplified due to forcing. In addition flow field investigations by means of instantaneous PIV-measurements were conducted to visualize the vortical

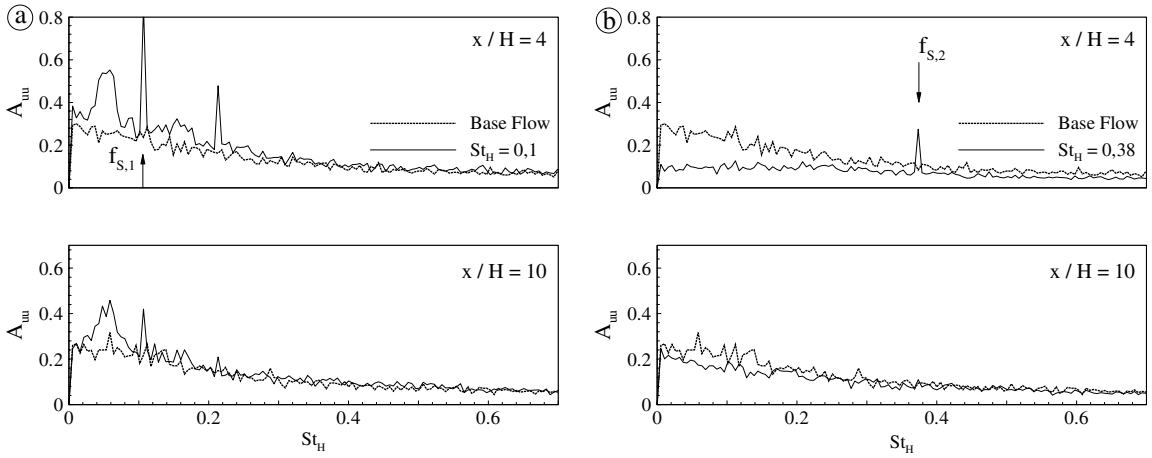

Fig. 5. Comparison of frequency spectra in the upper shear layer of a separation at a plane half diffuser with and without forcing: Excitation with vortex-shedding frequency ⓐ and with the initial shear layer instability frequency ⓑ.

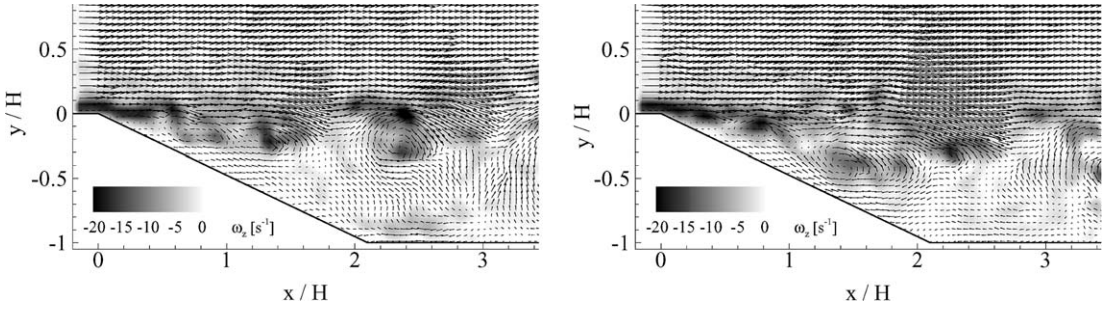

Fig. 6. Instantaneous PIV-measurements of the plane half diffuser flow (without forcing) show typical vortex structures in the shear layer.

structures (highlighted by the spanwise vorticity distribution in the vector field) according to the shear layer roll-up and the shedding of large scale vortices in the natural flow (Fig. 6). The corresponding Strouhal numbers, based on the slant height H, are $St_H = 0.1$ for the vortex-shedding and $St_H = 0.38$ for the initial shear layer instability. Based on the momentum thickness the Strouhal number of this shear layer instability is $St_\theta = 0.021$ and agrees with observations in other separated shear layers (e.g., Leder, 1992; Michalke, 1965).

The frequency response of forcing with the initial shear layer instability merely shows the forcing frequency itself as $x/H \leqslant 4$. Further downstream at $x/H = 10$ there is no noticeable effect. The fluctuation intensity is decreased compared to the base flow. This is confirmed by Fig. 7, where the RMS-value distribution of the velocity fluctuations is illustrated. The fluctuation intensity is significantly increased due to forcing with the vortex-shedding frequency (Fig. 5(a)). In those spectra an amplification of the forced structures is evident. Subharmonic frequencies also indicate that enlarged vortex structures emerge in the shear layer, leading to a significantly increased fluctuation intensity (Fig. 7(b)) and finally to an intensified momentum transfer from the recirculation to the flow outside of the separation bubble (e.g., Chapman et al., 1958).

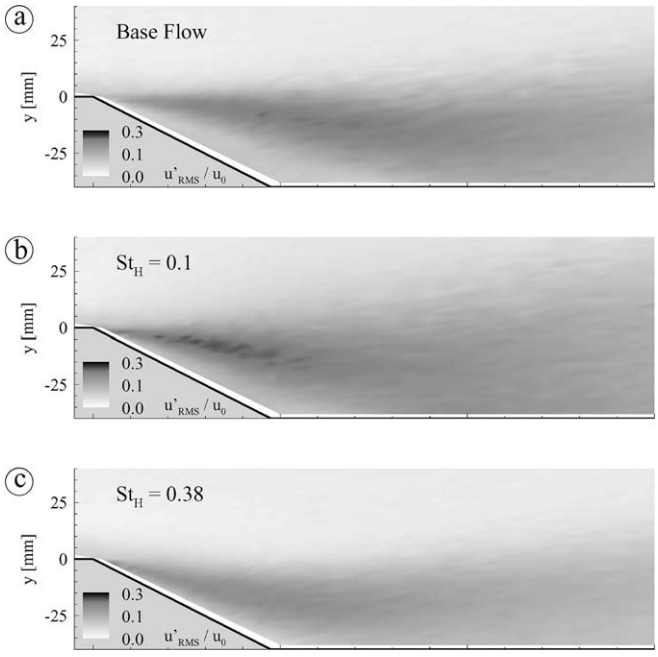

Fig. 7. Distribution of the velocity fluctuations behind a plane half diffuser.

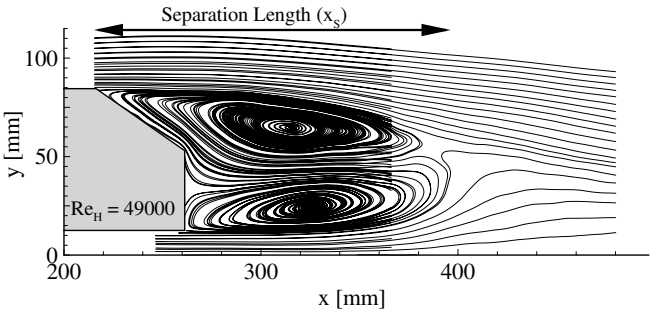

Fig. 8. Time-averaged flow field behind an ACM.

The forcing and amplification of large scale structures is obviously the most effective way to reduce flow separation in simple diffuser and bluff body configurations (Sigurdson, 1995; Kiya et al., 1997; Brunn and Nitsche, 2002, etc.) The next step is to apply this method to more complex and relevant engineering configurations. The ACM investigated in this study shows comparable streamwise flow structures in the near wake region, which is why the experiments focus on an unique approach to drag reduction in terms of active separation control. First of all, the unforced base flow was investigated with the time-averaged flow field in terms of streamlines shown in Fig. 8. Here, an ensemble average of 200 instantaneous PIV images is depicted. Flow structures typically occuring behind bluff bodies are visible (e.g., Leder, 1992): Two counter rotating vortex structures (time-averaged) and a stagnation point that closes the separation region. The overall separation length in this case is larger than compared to the original ACM (e.g., Ahmed et al., 1984), because of the more two-dimensional flow character in the near wake therefore a suppressed momentum transfer in spanwise direction.

Unlike a diffuser flow with a reattachment of the separated shear layer at the wall, two free shear layers collide in the wake behind bluff bodies and enclose a separation bubble. While the upper shear layer separates from the slant and is consequently driven by the slant configuration, the flow at the bottom is like a backward facing step flow. The exemplary snapshot of the instantaneous velocity field in Fig. 9 shows discrete structures of spanwise vortices. Typical wavelengths can be assigned to these structures, occurring in almost every instantaneous velocity field, and they scale with the slant height H. Hence, it is the obvious solution to force the flow and amplify these structures with frequencies according to shear layer instabilities. For this reason, a frequency range was chosen according to the Strouhal numbers $0.1 \leqslant St_H \leqslant 0.3$. Here, the lowest value corresponds to the vortex-shedding frequency estimated with the method of Kiya et al. (1997) and was confirmed through digital flow visualization documented by Brunn (2003). The initial shear layer instability primarily depends on the boundary layer conditions upstream of the separation point (Michalke, 1965; Leder, 1992) and was calculated to be around $St_\theta = 0.017$ ($St_H = 0.3$). All control experiments in the present study were performed with a forcing intensity of $c_\mu = 3 \times 10^{-3}$.

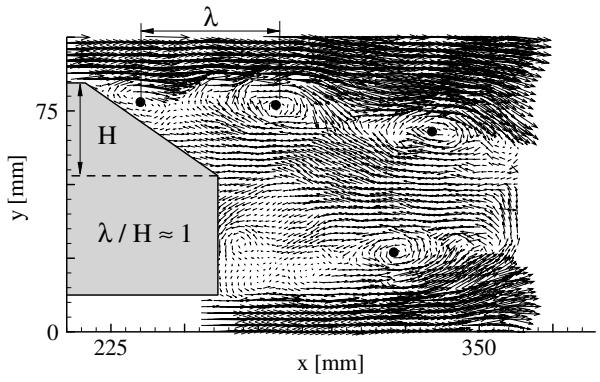

Fig. 9. Instantaneous velocity field behind an Ahmed car body with the characteristic wavelength of spanwise vortices.

A significant reduction of the turbulent car wake separation length was achieved in all forcing cases, but with noticeable difference in the resulting (mean) flow field (Fig. 10). The excitation with the vortex-shedding instability ($St_H = 0.1$, Fig. 10(b)) shows a drastic reduction of the recirculation area compared to the base flow (Fig. 10(a)). However, with increasing forcing frequency the forcing effectivity is consistently reduced and in the case of an excitation in the range of the shear layer instability ($St_H = 0.3$, Fig. 10(f)) the reduction is comparatively low.

The distribution of velocity fluctuations as seen in Fig. 7 for the half diffuser, is a reliable indicator for an enhanced momentum transfer by means of local forcing (Yoshioka et al., 1999). In Fig. 11 this distribution is depicted for forcing cases $0.1 \leqslant St_H \leqslant 0.3$, while Fig. 11(a) represents the flow without forcing. At frequencies close to the vortex-shedding the RMS-values far exceed that of the base flow. At $St_H = 0.3$ the distribution shows no significant enhancement and is comparable to the half diffuser investigations (Fig. 7). A closer look at Fig. 11(b) does not only show increased fluctuations in the slant region, but also goes to demonstrate that the momentum transfer in the near wake directly at the blunt end of the car is much more intensified than at other frequencies. As a result, the entrainment process starts much earlier and the forcing effect is stronger in the near wake region behind the car model.

The phase-averaged velocity fields given in Fig. 12 show the influence of the forcing in greater detail. The trigger information from the excitation mechanism was used for phase-averaged PIV measurements. After the postprocessing an average of 20 images for each phase was calculated. This figure depicts three exemplary phases in the range $0.4 \leqslant T \leqslant 0.8$. Exactly one forcing cycle is completed for $T = 1$ (see Fig. 4(c)). The left hand side shows the forcing with the vortex-shedding frequency, while on the right hand side the flow was excited with the initial shear layer instability. In addition to the streamlines, the value of the spanwise vorticity is marked. In both forcing cases an amplification of the vortex structure close to the slant edge obviously occurs immediately after the blowing phase

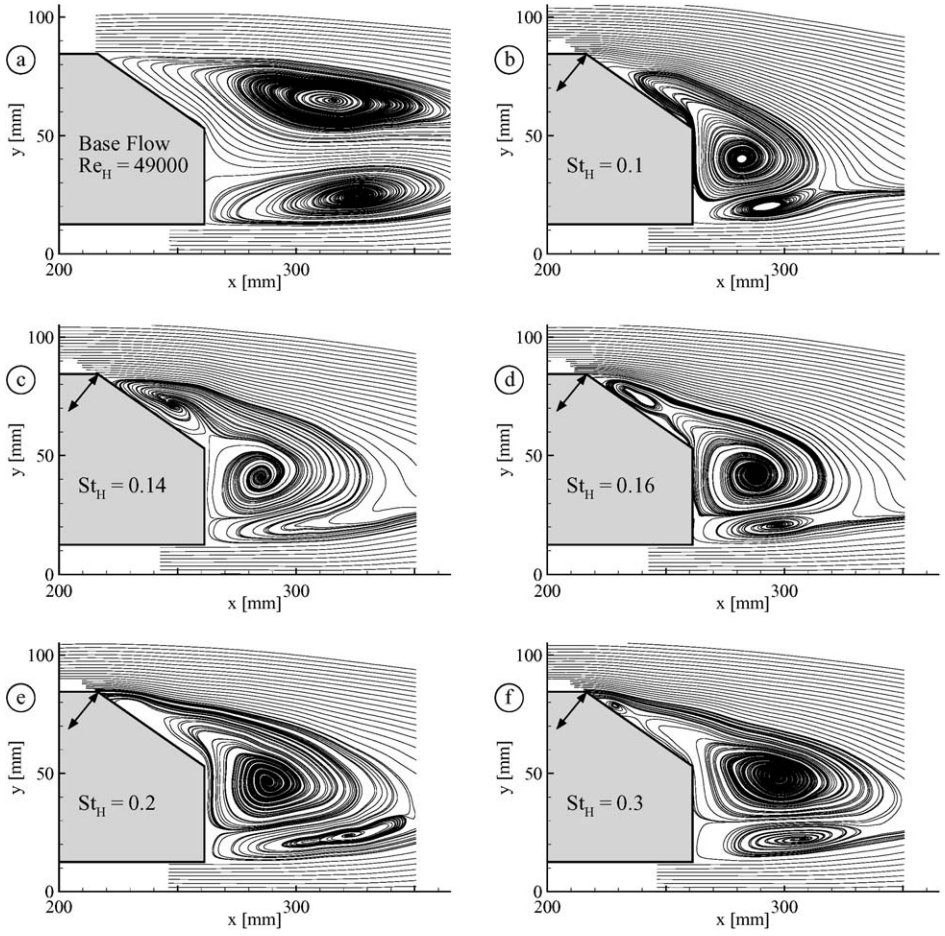

Fig. 10. Time-averaged flow fields behind an ACM.

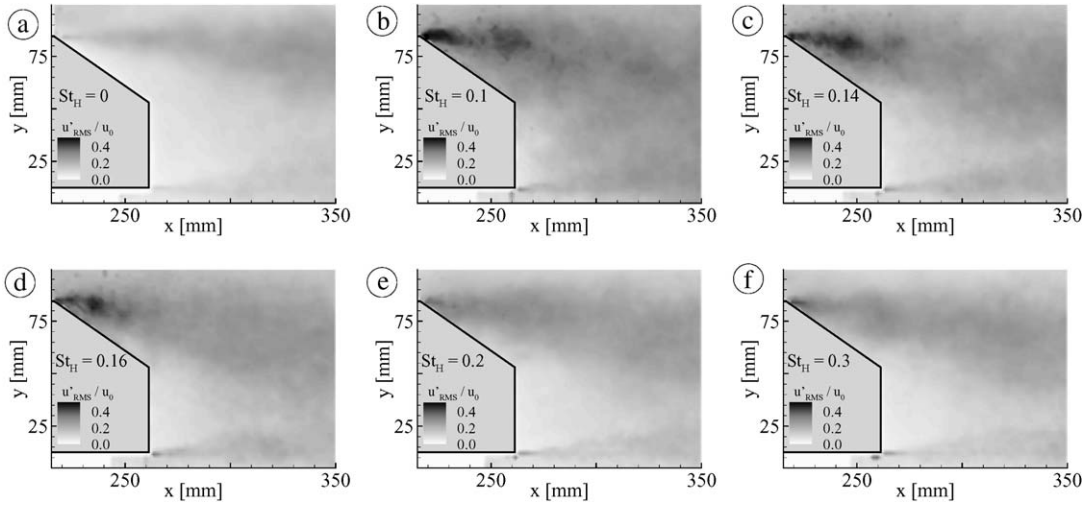

Fig. 11. Velocity fluctuations behind ACM.

(Fig. 12(a)). For forcing with $St_H = 0.3$ (Fig. 12(d)) this structure is very similar to those, observed in the instantaneous velocity field in Fig. 9. However, at the low frequency forcing this structure is enlarged up to the length of the slant. Further vortex growth at the high frequency forcing is comparable to the natural flow. The enlargement of the amplified vortex structure in the Fig. 12(a)–(c) exceeds the near wake region of the slant up to the blunt end of the car model. This is the main reason why the entrainment process in this case is much more intensified. Forcing with higher frequencies, especially with the initial shear layer instability, leads to a stabilization of the initial

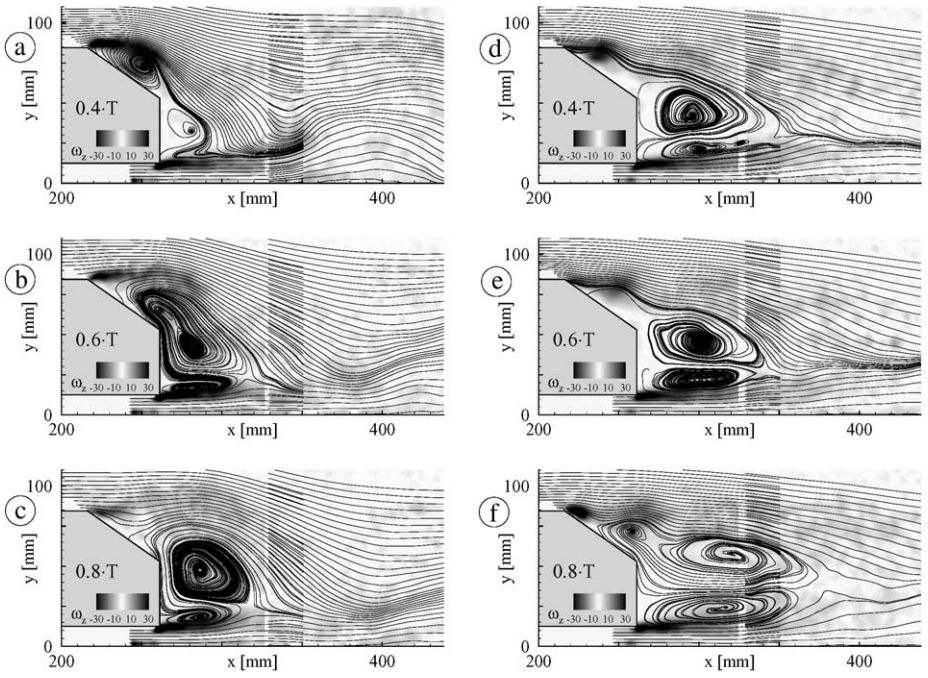

Fig. 12. Phase-averaged velocity fields due to local forcing: $St_H = 0.1$ (left side) and $St_H = 0.3$ (right).

vortex structure. This is indicated by the high local concentration of spanwise vorticity. Here, the fundamental wavelength could be found in almost every velocity field, whereas due to the low frequency forcing, the vortex structures grow rapidly and are hardly detectable further downstream. A closer look at the global flow field shows a significant oscillation of the upper shear layer. The amplitude of this oscillation is considerably higher than at the high frequency forcing. Consequently, the lower shear layer, separating from the bottom of the car model, can only be co-excited if the vortices are large enough and both shear layers interact. Both shear layers are connected with the vortex-shedding process (vortex-street). This proves that the combination of vortex-shedding and the enlarged entrainment due to amplified large vortex structures with a connected frequency is obviously the most effective mechanism to control such flow configurations.

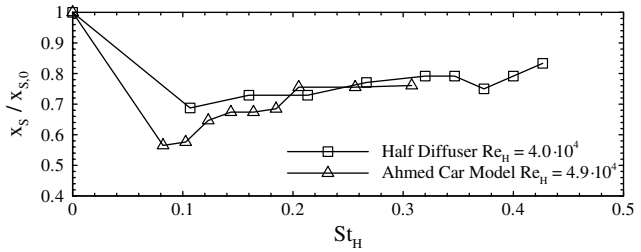

Fig. 13. Comparison of the reduced separation length depending on the forcing frequency for the two investigated configurations.

Fig. 13 summarizes the results achieved through investigations on active separation control for the two different flow configurations. The reduction of the time-averaged separation length for different forcing frequencies (Strouhal numbers) shown in this figure is normalized with the length

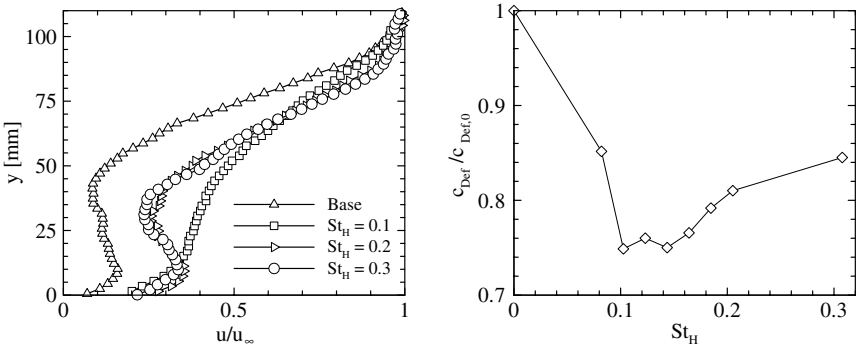

Fig. 14. Profiles of streamwise velocities $u(y)$ at $x = 420$ mm in the near wake of the ACM (left) and reduced coefficients of the velocity deficit depending on forcing Strouhal numbers (right).

of recirculation without forcing. The influence of different forcing intensities was not considered here, because of the strong shear layer receptivity to forcing frequencies and because of the power limit of the used actuator. An excitation with the frequency of vortex-shedding ($St_H = 0.1$) leads to a dramatically shorter separation bubble. With a higher forcing frequency the effect decreases because of the mechanisms explained above. The key to separation control in configurations similar to the two investigated here is the forcing and amplification of the dominating large scale vortices. The size of these vortices depends only on the geometry which causes the separation.

An analytical method to determine the vehicle drag and the drag coefficient c_D is the use of conservation of momentum with the velocity data of one upstream and at least one downstream position in the integration area far downstream Hucho (2002). The profiles of the streamwise velocity component at the downstream position $x = 420$ mm, depicted in Fig. 14 (left), already show a qualitative drag reduction. The velocity $u(y)$ in the near wake, normalized with the free stream velocity u_∞, is significantly increased due to the local forcing.

At this downstream position, an integral value of the velocity deficit was calculated. This one is equivalent to the profile drag coefficient. A velocity deficit in the measurement plane of $c_{Def} = 0.35$ was calculated for the unforced base flow, and it represents the profile drag of a two-dimensional configuration. Fig. 14 (right) summarizes the drag reductions in terms of a reduced velocity deficit achieved with the active separation control. An excitation with the frequency of vortex-shedding leads to a dramatic drag reduction in the excitation range $0.1 \leqslant St_H \leqslant 0.2$ (approximately 20%). The minimum drag ($c_{Def} = 0.25$) could be observed at $St_H = 0.1$. The effect decreases with higher forcing frequencies due to the mechanisms explained earlier.

4. Conclusions

The current study presents experimental investigations on active separation control by means of large scale vortex structure excitation and amplification. Actuators generating periodic perturbations to the flow were used to excite separated shear layers in two different geometrical configurations: a plane half diffuser and a two-dimensional generic car model configuration. Forcing frequencies in the range of the initial shear layer instability and the vortex-shedding were used to test the receptivity of the flow. An excitation in terms of periodical perturbations at the slant edge leads to increased velocity fluctuations in the shear layers, while the impulse transfer between the recirculation region and the outer flow was significantly intensified due to forcing at vortex-shedding frequencies. The most effective frequency for flow control, both for the plane half diffuser and for the ACM, was observed for the corresponding Strouhal number based on the slant height $St_H = 0.1$ of each. The amplified large scale vortices connected with the vortex-shedding process are the key to controlling the flow configurations investigated here.

Acknowledgement

This research was funded by the German Science Foundation (DFG) within the scope of the Sonderforschungsbereich Sfb 557, 'Control of Complex Turbulent Shear Flows'. This support is thankfully acknowledged by the authors.

References

Ahmed, S.R., Ramm, R., Faltin, G., 1984. Some salient features of the time-averaged ground vehicle wake. SAE-Techn. Paper Series, 840300.

Brunn, A., Nitsche, W., 2002. Separation Control in an Axisymmetric Diffuser Flow by Periodic Excitation. In: Rodi, W., Fueyo, N. (Eds.), Engineering Turbulence Modelling and Experiments, vol. 5. Elsevier Science, pp. 587–596.

Brunn, A., 2003. Aktive Beeinflussung abgelöster turbulenter Scherschichten in überkritischen Diffusoren mit Hilfe periodischer Anregung, TU Berlin, Ph.D. Thesis, Mensch und Buch Verlag.

Chapman, D.R., Kuehn, M., Larson, H.K., 1958. Investigations of Separated Flows with Emphasis on the Effect of Transition/NACA-Report 1356.

Hucho, W.-H., 2002. Aerodynamik der stumpfen Körper – Physikalische Grundlagen und Anwendung in der Praxis. Vieweg-Verlag.

Kiya, M., Shimizu, M., Mochizuki, O., 1997. Sinusoidal forcing of a turbulent separation bubble. J. Fluid Mech. 342, 119–139.

Krajnovic, S., Davidson, L., 2002. A Test Case for Large-Eddy Simulation in Vehicle Aerodynamics. In: Rodi, W., Fueyo, N. (Eds.), Engineering Turbulence Modelling and Experiments, vol. 5. Elsevier Science, pp. 47–657.

Leder, A., 1992. Abgelöste Strömungen – Physikalische Grundlagen. Vieweg-Verlag.

Lienhart, H., Stoots, C., Becker, S., 2002. Flow and Turbulence Structures in the Wake of a Simplified Car Model (Ahmed model). Notes on Numerical Fluid Mechanics, vol. 77. Springer, pp. 323–330.

Lin, J.C., Howard, F.G., Bushnell, D.M., Selby, B.V., 1990. Comparative Study of Control Techniques for Two-Dimensional Low-Speed Turbulent Flow Separation. In: Kozlov, A.V. (Ed.), Separated Flows and Jets. Springer, Berlin, pp. 429–474.

Michalke, A., 1965. Spatially growing disturbances in an inviscid shear layer. J. Fluid Mech. 23, 521–544.

Morel, T., 1978. The Effect of Base Slant Angle on the Flow Pattern and Drag of Three-Dimensional Bodies with Blunt Ends. In: Proc. of Symp. Aerod. Drag Mechanisms of Bluff Bodies and Road Vehicles. Plenum Press, New York, pp. 191–226.

Sigurdson, L.W., 1995. The structure and control of a turbulent reattaching flow. J. Fluid Mech. 298, 139–165.

Yoshioka, S., Obi, S., Masuda, S., 1999. Momentum transfer in the periodically perturbated turbulent separated flow over the Backward-Facing step. Proc. TSFP1, 1321–1326.